Journal of Medicinal and Nanomaterials Chemistry 1 (2022) 98-108

Journal of Medicinal and Nanomaterials Chemistry

Journal homepage: https://jmnc.samipubco.com/

Original Research Article

Investigation of magnetic properties of Fe_3O_4/Halloysite nanotube/polypyrrole core-shell nanocomposite and its stability in the acidic environment

Sajjad Tabar Maleki*, Seyed Javad Sadati

Department of Physics, Iran University of Science and Technology, Tehran16846-13114, Iran

ARTICLE INFORMATION

Received: 18 January 2022
Received in revised: 9 March 2022
Accepted: 13 March 2022
Available online: 2 March 2022

DOI: 10.48309/JMNC.2022.2.2

KEYWORDS

Halloysite nanotube
Polypyrrole
Acid stability
Magneti

ABSTRACT

In this research study, Fe_3O_4 nanoparticles and Fe_3O_4/Halloysite nanotubes (HNTs) were initially prepared for testing using a co-precipitation method. Fe_3O_4/HNTs/polypyrrole (PPy) core-shell magnetic nanocomposite was synthesized using in situ polymerization of pyrrole monomers at the Fe_3O_4/HNT level. The Fourier transform spectrum revealed well the characteristic Halloysite and PPy peaks. Scanning electron microscopy images showed the uniform structure of nanoparticles and nanocomposite. The change in nanoparticle diameter after polymerization was well visible. Fe_3O_4/HNTs/PPy nanocomposites have strong acids' fine dispersion and stability properties, making them suitable for various applications. Measurement of magnetic at room temperature showed that Fe_3O_4 and Fe_3O_4/HNTs nanoparticles have a magnetic saturation of 73.84 emu/g and 30.63 emu/g, respectively. Coating the nanoparticles with PPy reduces the saturation magnetization value of Fe_3O_4/HNTs/PPy nanocomposites to 6.7 emu/g. Results illustrated that Fe_3O_4/HNTs/PPy nanocomposites have great potential for performing applications.

Corresponding author, email: s_tabarmaleki@physics.iust.ac.ir (S.T. Maleki).

Graphical Abstract

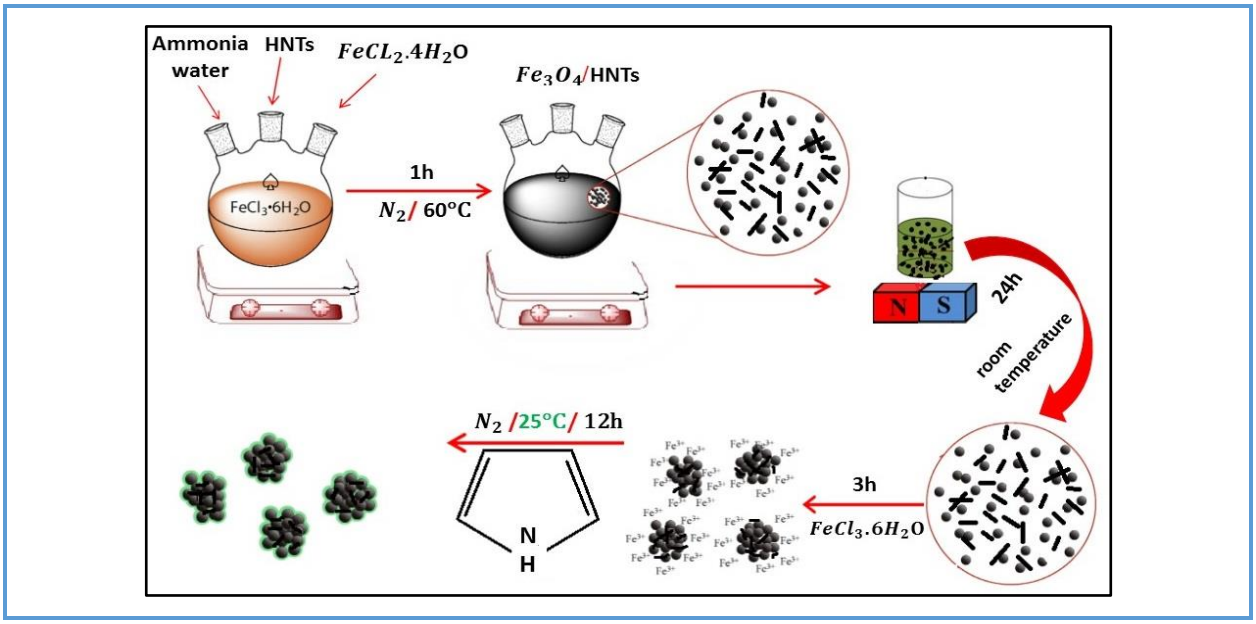

Introduction

In recent years, nanometer-sized composite materials have been widely used due to their excellent electrical and magnetic properties. [1–3]. Magnetite is one of the most important nanoparticles with various applications that received much attention due to its unique physical and chemical properties. Therefore, magnetic nanoparticles have different applications in the field of photocatalysts, microwave absorption, drug delivery, and MRI [2–7]. In this case, Fe_3O_4 nanoparticles are easily affected by acid corrosion or air oxidation and are easily collected in an aqueous system in a harsh environment. Fe_3O_4 nanoparticles do not have an effective surface modification and stabilization strategy, which reduces their applications. It is necessary to achieve the desired result to adjust the surface performance of Fe_3O_4 nanoparticles as much as possible. To improve the properties of nanoparticles and make nanocomposites with unique properties, the use of magnetite nanoparticles with polymers is one of the best possible methods [8, 9]. HNTs is a natural microporous nanotube that can enhance the ability of PPy to load nanoparticles [10]. In addition to their microporous properties, these nanotubes have high mechanical and thermal stability, low toxic structure, and green properties, which has caused a lot of attention to them [11]. HNTs with non-intertwined properties and rod geometry have made them readily dispersible in solutions or polymer matrices [12]. Polymer shell prevents the accumulation and corrosion of the magnetic core as much as possible. With this method, nanocomposites with excellent electrical and magnetic properties can be easily prepared and used in various fields. PPy as a conductive polymer has attracted much attention due to its good electrical conductivity, relatively easy preparation, and excellent environmental stability [13–15]. In this research, we first synthesized Fe_3O_4 and Fe_3O_4/HNTs nanoparticles using the co-precipitation method, and in the next step, Fe_3O_4/HNTs/PPy core-shell nanocomposite prepared using in situ polymerization.

Meanwhile, the stability of nanoparticles and nanocomposites studied the environment in a

strongly acidic way. Results showed that Fe_3O_4/HNTs/PPy nanocomposites have good stability. Finally, the magnetic properties of the synthesized materials were investigated.

Experimental

Materials and method

Pyrrole monomer and Halloysite nanotube (HNTs) received from Sigma–Aldrich. Ammonia (NH3), $FeCl_2.4H_2O$, and $FeCl_3.6H_2O$ were purchased from Merck. Hydrochloric acid (HCL) was also purchased from Nirouchlor.

Synthesis of Fe_3O_4 nanoparticles

The co-precipitation method utilized to prepare Fe_3O_4 nanoparticles [16]. First, 0.4 g ($FeCl_2.4H_2O$) and 1.16 g ($FeCl_3.6H_2O$) were added to 200 mL of distilled water under nitrogen gas in a two-port balloon and stirred at 60 °C. 30 min after the start of the process, ammonia solution (20 mL) was added dropwise to the initial solution for 2 h, after which the color of the solution changed to black. The stirring process took about 2 h to obtain a uniform mixture.

Synthesis of Fe_3O_4/HNTs nanocomposite

Initially, 0.4 g of halloysite, 0.4 g ($FeCl_2.4H_2O$), and 1.16 g ($FeCl_3.6H_2O$) were added to 200 mL of distilled water under nitrogen gas in a two-port balloon and stirred at 60 °C. 30 min after the start of the process, ammonia solution (20 mL) was added dropwise to the initial solution, which became more pronounced with each drop of the color change of the solution to black. The moving process took about 2 h to obtain a uniform mixture [17].

Synthesis of Fe_3O_4/HNTs /PPy

Initially, 0.2 g of the synthesized nanoparticles (Fe_3O_4/Halloysite) were mixed in 50 mL of distilled water for 10 min. Next, 3 g of $FeCl_3.6H_2O$ was added to the solution according to the polymerization process. After 3 hours, 0.3 mL of pyrrole monomer was added dropwise to this solution and stirred under nitrogen gas for 12 h. At the end of this period, the synthesized nanocomposite was separated using a magnet, as shown in Figure 1.

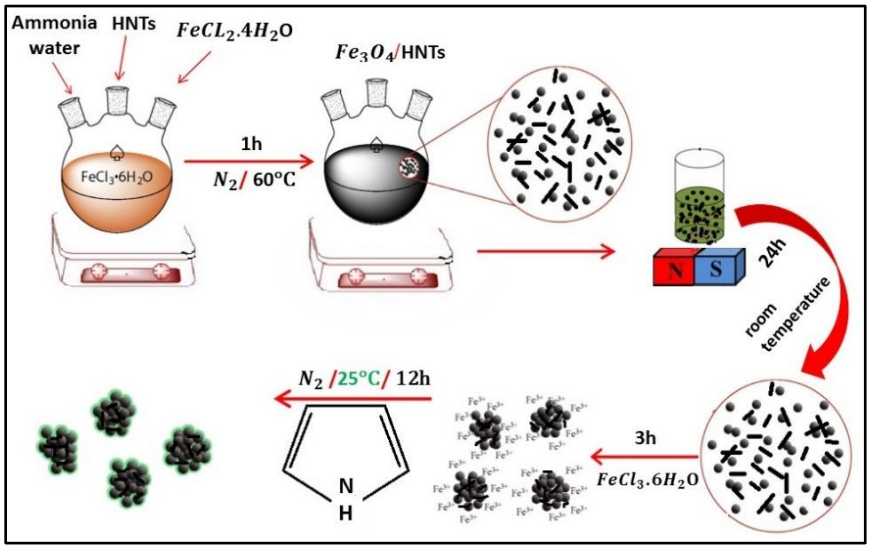

Figure 1. Schematic of Fe_3O_4/HNTs/PPy nanocomposite synthesis

Characterization

Fourier transform infrared spectroscopy (FTIR) was taken with Shimadzu FTIR-8400S Spectrometer. Scanning electron microscopy (SEM) images were taken using VEGA-TESCAN. The energy dispersive X-Ray (EDX) analysis was obtained using a Shimadzu EDX-700 instrument. Thermogravimetric analysis (TGA) was performed using a Bahr-STA 504 device. X-ray diffraction (XRD) patterns were recorded by an X' Pert Pro X-ray diffractometer. Soluble pH was measured using a TES-1381 pH meter. The vibrating sample magnetometer (VSM) cure analysis was performed using a VSM device, the LBKFB model.

Results and Discussion

The XRD test was used for the characterization of nanocomposites (). The obtained XRD pattern of the nanocomposites revealed the dominant amorphous structures and was approximately similar to XRD pattern of the pure PPy and Halloysite. The pattern showed that the amorphous PPy matrix coats the Fe_3O_4 nanoparticles, and therefore, their peaks did not appear (Figure 2). This result agrees with the reported result of similar work by Chen and co-workers [18].

The FTIR spectra of samples of HNTs, Fe_3O_4/HNTs, and Fe_3O_4/HNTs/PPy nanocomposites are well illustrated in Figure 3**a–c**. Deformation of Si-O-Si and Al-O-Si can be observed in the vicinity of peaks 467 and 536 cm^{-1}, respectively. The O-H deformation of the internal hydroxyl groups can be observed in the vicinity of the 910 cm^{-1} peaks. Peaks close to 1000 cm^{-1} are related to Si-O groups in HNTs (Figure 3**a**) [19]. The broadband at 1639 cm^{-1} is related to the bending vibration of internally absorbed water and crystallization water in HNTs [20]. Peaks neer to 3622 and 3692 cm^{-1} are caused by the stretching vibrations of the hydroxyl groups of the inner surface of HNT [21]. According to Figure 3**b**, the vibration traction of the hydroxyl groups of iron oxide causes broadband at 3430 cm^{-1} [22]. The vibration of the Fe-O band causes a peak at 580 cm^{-1}. The chemical composition of PPy was confirmed by the presence of peaks near 907, 1034, and 1308 cm^{-1} [23]. Peak near 1466 cm^{-1} ensures the pyrrole ring. The 1543 cm^{-1} peak shows the conjugate C-N stretching. The presence of out-of-plane vibrations C-H and ring deformation confirmed, despite peaks near 927 and 1045 cm^{-1}. Figure 3**c** shows that Fe_3O_4/HNTs/PPy nanocomposite has Fe_3O_4 and PPy-defining peaks.

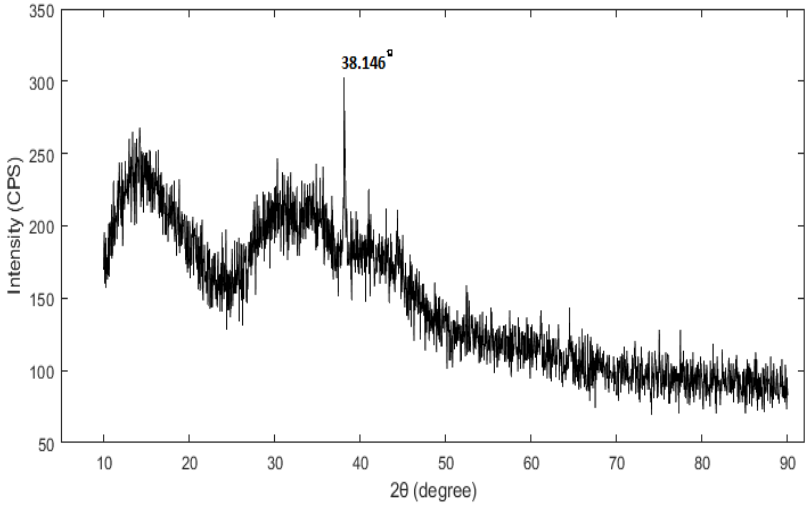

Figure 2. X-ray diffraction spectrum of nanocomposites Fe_3O_4/HNTs/PPy

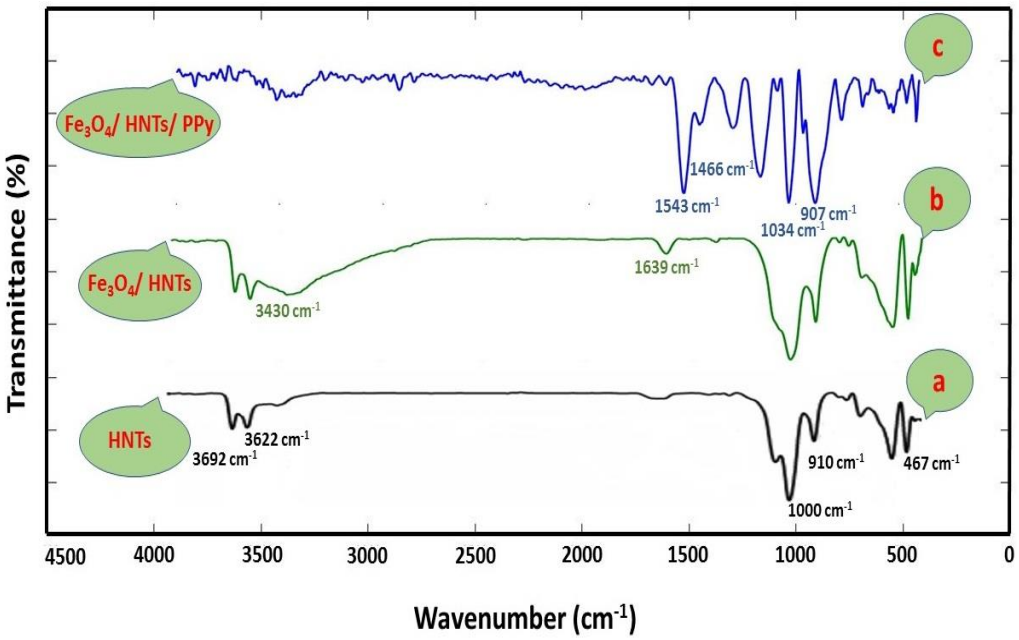

Figure 3. FT-IR spectra of the Prepared samples a) Halloysite, b) Fe_3O_4/Halloysite, and c) Fe_3O_4/Halloysite/Polypyrrole nanocomposites

SEM images of the nanocomposites are well visible in Figure 4. The formation and presence of Fe_3O_4 on halloysite nanotubes are visible in Figure 4**a** and **b**. Magnetic nanoparticles have accumulated among the nanoparticles due to the force of gravity. As you see in Figure 4**c** and **d**, the formation of a polymer coating on nanoparticles is due to polymerization. The size of magnetic nanoparticles on halloysite nanotubes is from 30 to 70 nm, which after polymerization and polymer coating, the particle size increases.

Figure 5 shows the EDX analysis of the synthesized nanocomposite, which confirms the presence of iron, nitrogen, aluminum, silicon, oxygen, and carbon elements in the nanocomposite. This result means that the prepared nanocomposite has acceptable conditions and quality. HNTs have the structural formula $Al_2Si_2O_5(OH)_4$. The presence of aluminum and silicon is well illustrated in the analysis. The presence of other elements that are evidence for the existence of magnetic particles Fe_3O_4 and pyrrole can be seen in the peaks of Fe, O, N, and C.

The TGA results of the nanocomposite are shown in Figure 6. At 110 °C, the weight of the sample is reduced by about 4% due to the loss of moisture in the polymer [24, 25]. At temperatures above 220 °C, PPy is degraded, so at 250 °C, the weight is reduced by about 12%. Decomposition of PPy begins at temperatures above 250 °C, which reduces the weight of the nanocomposite by about 52% to 600 °C. Loss of C, H, and N in PPy is one of the leading causes of weight loss. The sharp decrease in mass is due to the thermal degradation of PPy chains, which at a temperature of 300 °C, the weight of the sample is sharply reduced [26]. Fe_3O_4 nanoparticles have excellent stability up to 750 °C [27]. At 480 to 640 °C, dehydroxylation of halloysite occurs [28]. For this reason, the main factor in reducing the weight of Fe_3O_4/HNTs/PPy nanocomposite is the attendance of PPy and halloysite nanotubes.

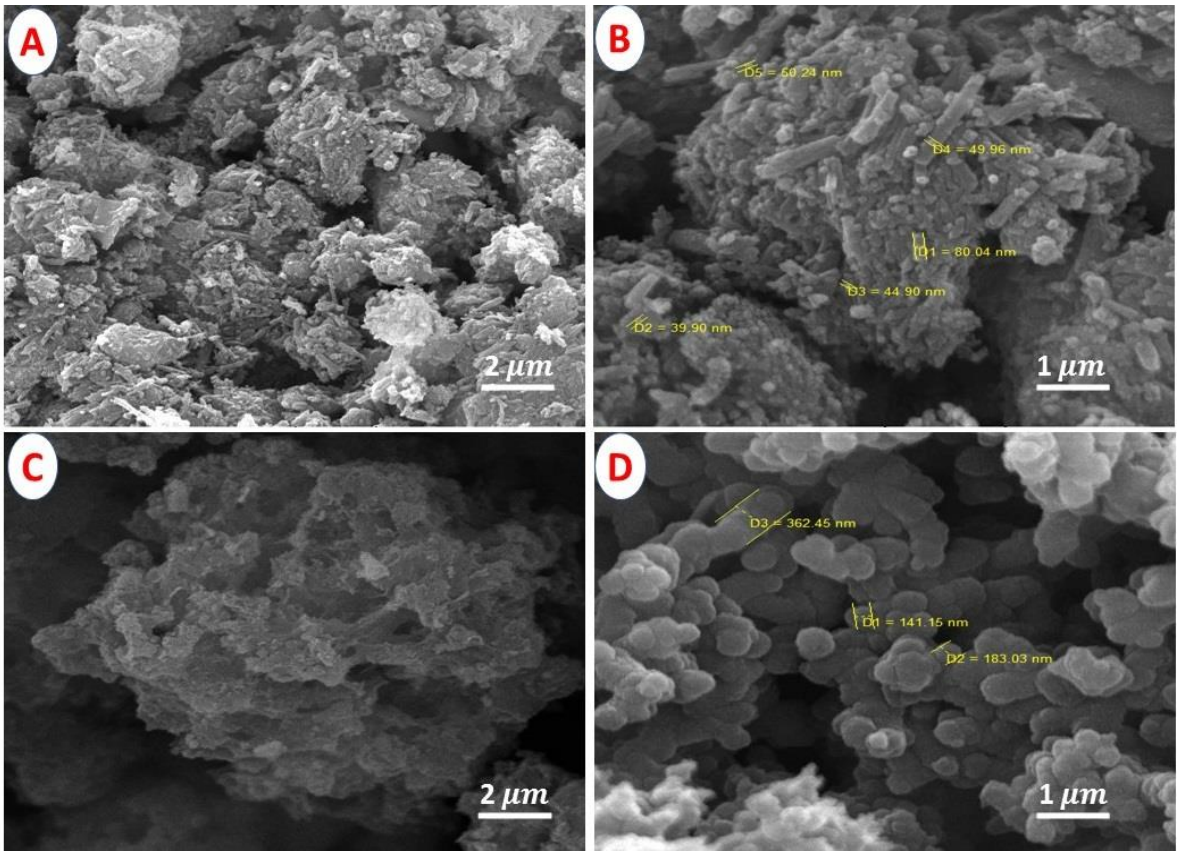

Figure 4. SEM images of synthesized materials

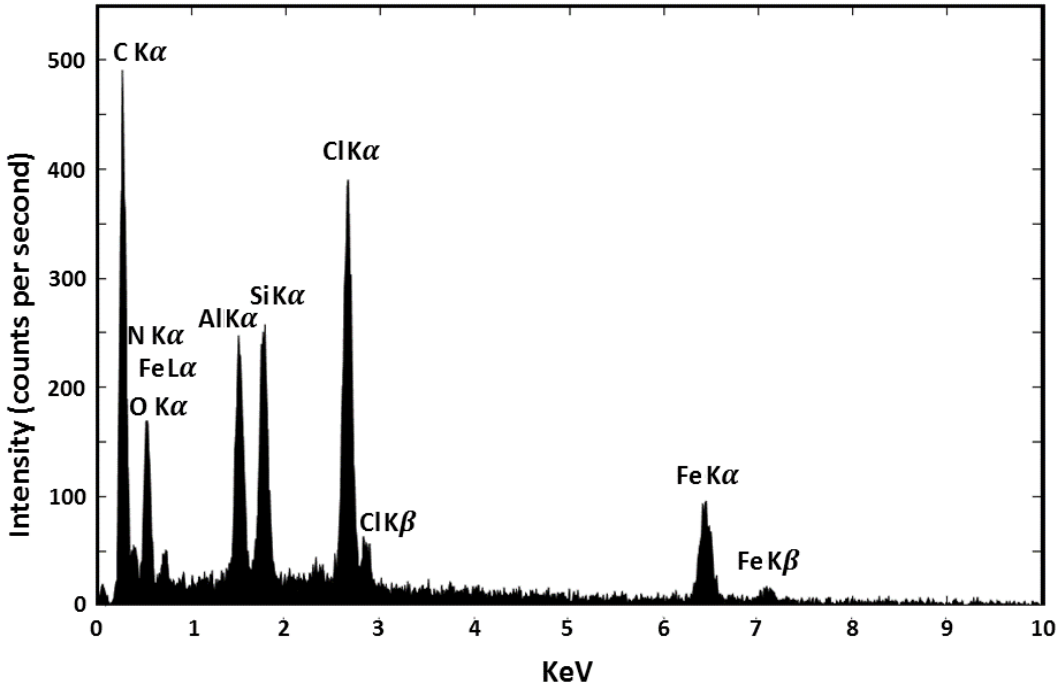

Figure 5. EDX analysis of the Fe_3O_4/Halloysite/Polypyrrole nanocomposite

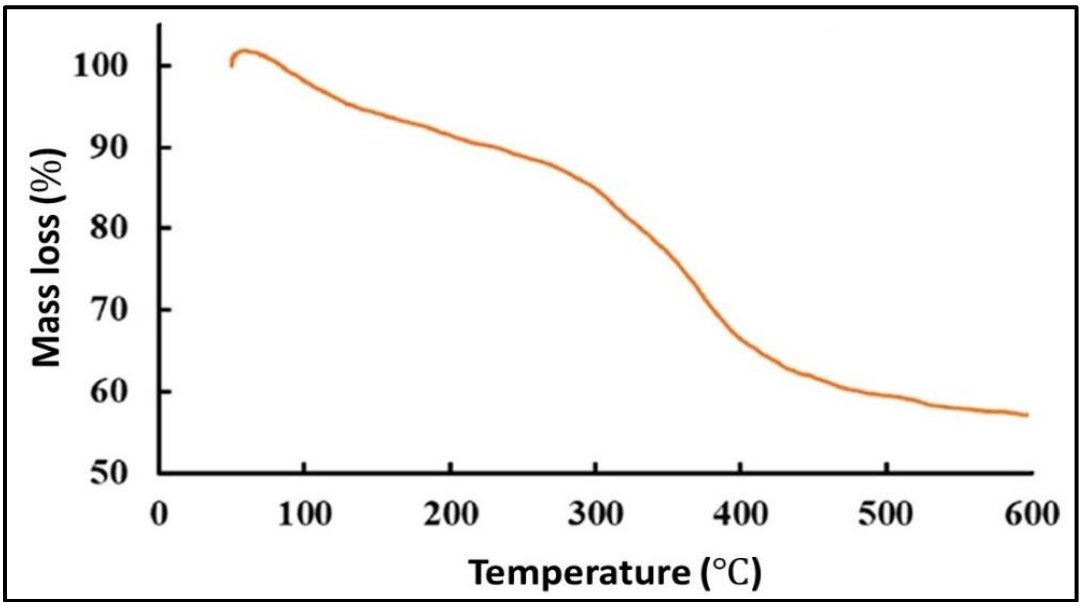

Figure 6. TGA thermograms of Fe_3O_4/Halloysite/Polypyrrole nanocomposite

Evaluation of nanocomposite stability in the acidic environment

The acid stability of Fe_3O_4/HNTs/PPy nanocomposite is one of the crucial factors that should be considered because it plays a vital role in applying this nanocomposite. Decomposition of PPy in an acidic medium causes the Fe_3O_4/HNTs/PPy nanocomposite to degrade. Fe_3O_4 nanoparticles and Fe_3O_4/HNTs/PPy nanocomposite were tested To evaluate acid stability in a strongly acidic environment. Figure 7**a** shows that 7 mL of HCl solution (0.1 M) was used for this experiment. This amount of acid was added to the bottles containing Fe_3O_4 nanoparticles and Fe_3O_4/HNTs/PPy nanocomposites, respectively, to investigate the corrosion effect. After 15 minutes from the start of the experiment, the solution containing Fe_3O_4 nanoparticles is slowly etched, and the color of the solution gradually changes. The solution includes Fe_3O_4/HNTs/PPy, the nanocomposite has maintained its stability, and the color of the solution has not changed. After several hours (from 3 hours to 12 hours), Fe_3O_4 nanoparticles are almost completely etched by HCl acid, which is confirmed by the bright yellow color of the solution. While the corrosion of Fe_3O_4/HNTs/PPy is barely visible after 24 h, this indicates that the Fe_3O_4/HNTs/PPy nanocomposite is highly stable against a strong acid medium. As seen in Figure 7**b**, according to the pH-time curve, the pH value of the acidic solution containing Fe_3O_4 nanoparticles increases rapidly after 15 min from the start of the experiment, while the solution contains the Fe_3O_4/HNTs/PPy nanocomposite has a stable pH value even after 24 h which has increased slightly. The PPy shell has also been shown to be strong sufficient to protect the Fe_3O_4 from acid corrosion [29]. The results of this experiment also show that both Fe_3O_4 nanoparticles and Fe_3O_4/HNTs/PPy nanocomposites have better stability than the experiment performed by Tang *et al*. This could be due to the synthesis method, the materials used as well as the halloysite nanotubes [30].

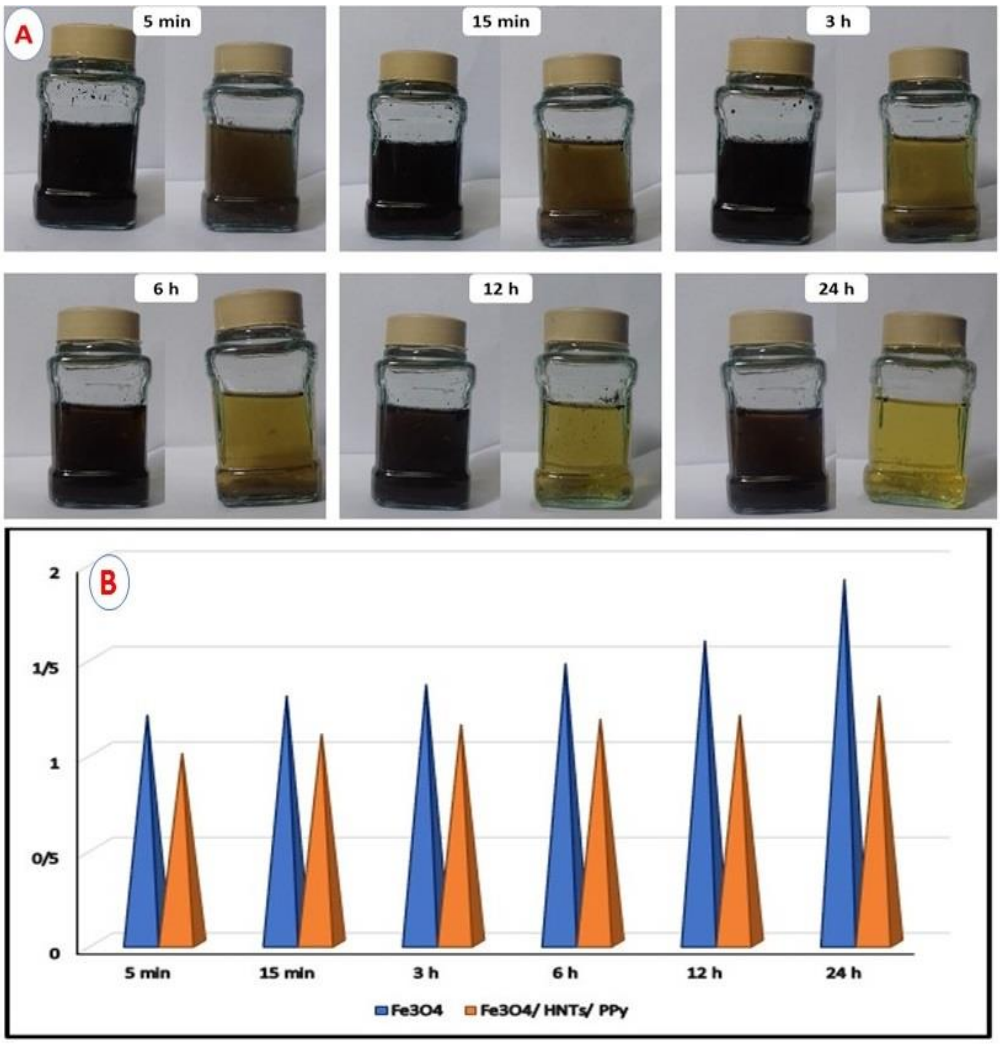

Figure 7. a) Acid stability analysis of Fe_3O_4/Halloysite nanotube/Polypyrrole and pure Fe_3O_4 (left: Fe_3O_4/Halloysite nanotube/Polypyrrole, right: Fe_3O_4, and b) pH diagram of dispersion of samples in HCl (0.1 M) at different times

Figures 8 and 9 show the VSM analysis of Fe_3O_4, Fe_3O_4/HNTs, and Fe_3O_4/HNTs/PPy. As shown in Figure 8**a** and **b**, Fe_3O_4 and Fe_3O_4/HNTs nanoparticles have a magnetic saturation of 73.84 emu/g and 30.63 emu/g, respectively. According to the obtained results, the magnetic property of Fe_3O_4 nanoparticles is significantly reduced with the addition of halloysite nanotubes. By performing the polymerization process and adding PPy, the magnetic property of Fe_3O_4/HNTs/PPy nanocomposites is reduced. The magnetic saturation of the nanocomposite is 6.7 emu/g, as shown in Figure 9. VSM analysis shows that the Fe_3O_4/HNTs/PPy nanocomposite is a soft magnetic material easily magnetized by exposure to a magnetic medium. The presence of non-magnetic polymers and HNTs on the surface of magnetic nanoparticles significantly reduces the magnetic properties of Fe_3O_4/HNT and Fe_3O_4/HNTs/PPy nanocomposites. PPy and HNTs significantly decrease the magnetic saturation property [31].

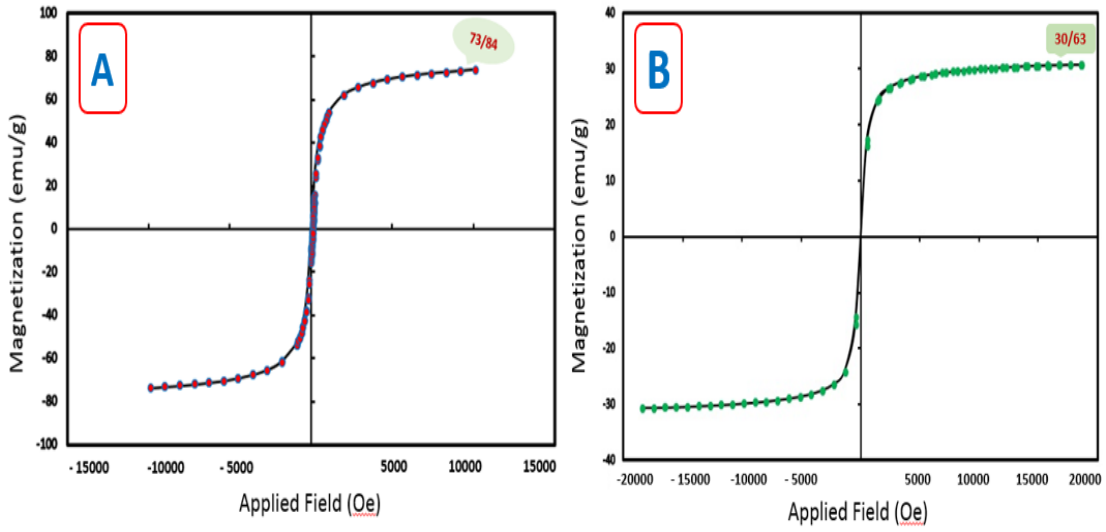

Figure 8. VSM magnetization curve of a) Fe_3O_4 and b) Fe_3O_4/HNTs

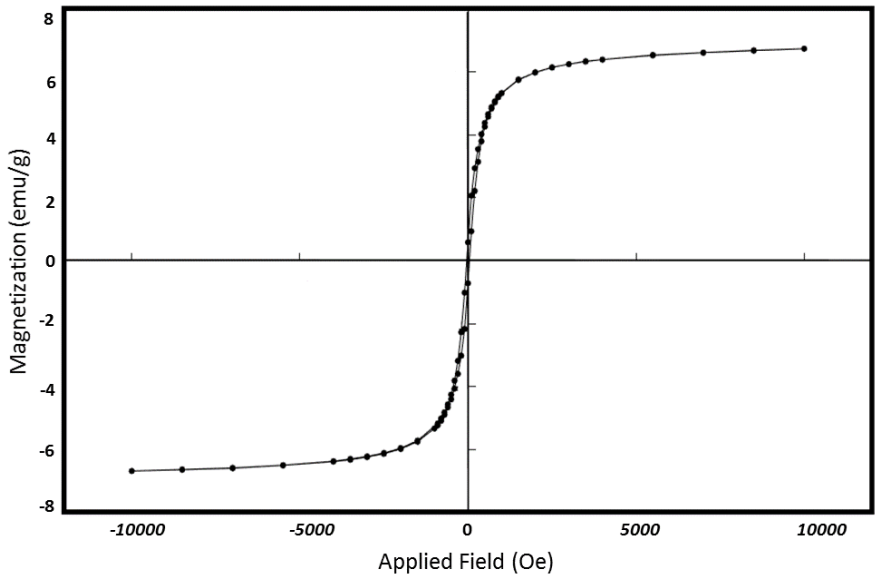

Figure 9. VSM magnetization curve of Fe_3O_4/ HNTs /PPy nanocomposite

Conclusions

In summary, we first prepared Fe_3O_4 and Fe_3O_4/HNTs nanoparticles using the co-precipitation method and then synthesized Fe_3O_4/HNTs/PPy core-shell nanocomposite using the in-situ polymerization method. Fe_3O_4/HNTs/PPy nanocomposites were not etched for 24 h in an HCl solution (0.1 M) at room temperature. This result indicates that Fe_3O_4/HNTs/PPy nanocomposites are very stable in acidic areas. The result makes this nanocomposite have many applications. Magnetic hysteresis ring measurements revealed that Fe_3O_4/HNTs/PPy core-shell nanocomposite is a soft magnetic material easily magnetized by exposure to a magnetic medium.

Acknowledgments

The authors are highly grateful for the support of the Research Council of Iran University of Science and Technology.

Disclosure Statement

No potential conflict of interest was reported by the authors.

Orcid

Sajjad Tabar Maleki 0000-0001-7612-1093

Seyed Javad Sadati 0000-0001-9772-7422

References

[1]. Su N., Li H.B., Yuan S.J. *Express Polym Lett*., 2012, **6**:697 [Crossref], [Google Scholar], [Publisher]

[2]. Oka C., Ushimaru K., Horiishi N., Tsuge T., Kitamoto Y. *Journal of Magnetism and Magnetic Materials*, 2015, **381**:278 [Crossref], [Google Scholar], [Publisher]

[3]. Buyuksagis A., Kara S., Aksut A.A. *Prot. Met. Phys Chem. Surf.*, 2015, **51**:155 [Crossref], [Google Scholar], [Publisher]

[4]. Wang S.Q., Zhang J.Y., Chen C.H. *J. Power. Sources*, 2010, **195**:5379 [Crossref], [Google Scholar], [Publisher]

[5]. Cao H.Q., Liang R.L., Qian D., Shao J., Qu M.Z. *J. Phys. Chem. C*, 2011, **115**:24688 [Crossref], [Google Scholar], [Publisher]

[6]. Sasidharan M., Gunawardhana N., Yoshio M., Nakashima K. *Ionics*, 2013, **19**:25 [Crossref], [Google Scholar], [Publisher]

[7]. Rouhi M., Babamoradi M., Hajizadeh Z., Maleki A., Tabar Maleki S. *Optik*, 2020, **212**:164721 [Crossref], [Google Scholar], [Publisher]

[8]. Chen Y., Xia H., Lu L., Xue J.M. *J. Mater. Chem*, 2012, **22**:5006 [Crossref], [Google Scholar], [Publisher]

[9]. Mylkie K., Nowak P., Rybczynski P., Ziegler-Borowska M. *Materials*, 2021, **14**:248 [Crossref], [Google Scholar], [Publisher]

[10]. Li L., Wang F., Lv Y., Liu J., Zhang D., Shao Z. *Appl. Clay Sci*, 2018, **161**:225 [Crossref], [Google Scholar], [Publisher]

[11]. Papoulis D. *Appl. Clay Sci*, 2019, **168**:164 [Crossref], [Google Scholar], [Publisher]

[12]. Xie Y., Chang P.R., Wang S., Yu J., Ma X. *Carbohydr. Polym*., 2011, **83**:186 [Crossref], [Google Scholar], [Publisher]

[13]. Li Y., Chen G., Li Q., Qiu G., Liu X. *J. Alloys. Compd*., 2011, **509**:4104 [Crossref], [Google Scholar], [Publisher]

[14]. Small C.J., Too C.O., Wallace G.G. *Polymer Gels and Networks*, 1997, **5**:251 [Crossref], [Publisher]

[15]. Ramya R., Sivasubramanian R., Sangaranarayanan M.V. *Electrochim. Acta.*, 2013, **101**:109 [Crossref], [Google Scholar], [Publisher]

[16]. Maleki A., Hajizadeh Z., Firouzi-Haji R. *Micropor. Mesopor. Mater.*, 2018, **259**:46 [Crossref], [Google Scholar], [Publisher]

[17]. Kadama A.A., Sung J.S., Sharma B. *Journal of Alloys and Compounds*, 2021, **854**:157041 [Crossref], [Google Scholar], [Publisher]

[18]. Chen J., Feng J., Yan W. *Journal of Colloid and Interface Science*, 2016, **475**:26 [Crossref], [Google Scholar], [Publisher]

[19]. Tierrablanca E., Romero-García J., Roman P., Cruz-Silva R. *Appl. Catal. A*, 2010, **381**:267 [Crossref], [Google Scholar], [Publisher]

[20]. Song X., Zhou L., Zhang Y., Chen P., Yang Z. *J. Clean. Production*, 2019, **224**:573 [Crossref], [Google Scholar], [Publisher]

[21]. Luo P., Zhao Y., Zhang B., Liu J., Yang Y., Liu J. *Water. Res.*, 2010, **44**:1489 [Crossref], [Google Scholar], [Publisher]

[22]. Hsieh S., Huang B.Y., Hsieh S.L. *Nanotechnology*, 2010, **21**:445 [Google Scholar], [Publisher]

[23]. Yang R.B., Reddy P.M., Chang C.J., Chen P.A., Chen J.K., Chang C.C. *Chem. Eng. J*., 2016, **285**:497 [Crossref], [Google Scholar], [Publisher]
[24]. Mavinakuli P., Wei S., Wang Q., Karki A., Dhage S.R., Wang Z., Young D., Guo Z. *J. Phys. Chem. C*, 2010, **114**:3874 [Crossref], [Google Scholar], [Publisher]
[25]. Shin K., Karki A.B., Young D.P., Kaner R.B., Hahn H.T. *J. Nanopart. Res*., 2009, **11**:1441 [Crossref], [Google Scholar], [Publisher]
[26]. Jang J., Yoon H. *Adv. Mater.*, 2004, **16**:799 [Crossref], [Google Scholar], [Publisher]
[27]. Rajesh U.C., Divya, Rawat D.S. *RSC Adv.*, 2014, **4**:41323 [Crossref], [Google Scholar], [Publisher]
[28]. Kadi S., Lellou S., Marouf-Khelifa K., Schott J., Gener-Batonneau I., Khelifa A. *Micropor. Mesopor. Mater.*, 2012, **158**:47 [Crossref], [Google Scholar], [Publisher]
[29]. Kim Y.H., Sim B., Choi H.J. *Colloids. Surf. A*, 2016, **507**:103 [Crossref], [Google Scholar], [Publisher]
[30]. Tang S., Lan Q., Liang J., Chen S., Liu C., Zhao J., Cheng Q., Cao Y. C., Liu J. *Materials and Design*, 2017, **121**:47 [Crossref], [Google Scholar], [Publisher]
[31]. Li Y., Chen G., Li Q., Qiu G., Liu X. *J. Alloys. Compd*., 2011, **509**:4104 [Crossref], [Google Scholar], [Publisher]

How to cite this manuscript: Sajjad Tabar Maleki*, Seyed Javad Sadati. Investigation of magnetic properties of Fe_3O_4/Halloysite nanotube/polypyrrole core-shell nanocomposite and its stability in the acidic environment. *Journal of Medicinal and Nanomaterials Chemistry*, 4(2) 2022, 98-108. DOI: 10.48309/JMNC.2022.2.2